ISSN (Print) 1226-1750
ISSN (Online) 2233-6656
Journal of Magnetics 26(2), 162-165 (2021) https://doi.org/10.4283/JMAG.2021.26.2.162

Tunability of Magnetism: An Interplay of Magnetic Anisotropy and Magnetoelasticity

Qurat-ul-Ain, Soon Cheol Hong*, and S. H. Rhim*

Department of Physics and Energy Harvest-Storage Research Center, University of Ulsan, Ulsan 44610, Republic of Korea

(Received 11 January 2021, Received in final form 21 May 2021, Accepted 25 May 2021)

We present theoretical study on spin reorientation transition (SRT). A phenomenological model is provided, which treats magnetic energy as sum of magnetoelasticity, magnetocrystalline anisotropy, and demagnetization contributions. We show that critical strain exists by analytically solving the phenomenological model, as a consequence of an interplay between aforementioned contributions. For more quantitative understanding, numerical estimate is performed for thin FePt and $Fe_{60}Co_{40}$ films, where experimentally accessible critical strain is 2 %. Further, this feasible strain is due to the large magnetoelastic coefficient (b_1) and the optimal saturation magnetization, which is not achievable in thin Fe film.

Keywords : spin reorientation transition, magnetic anisotropy, magnetoelasticity, thickness effect, FePt, $Fe_{60}Co_{40}$

1. Introduction

In study of magnetism, magnetic thin films have been favorite for offering interesting properties distinct from their bulk counterparts [1]. Due to recent progress in magnetic devices [2-4], thin films have attracted in many aspects. The reduced dimensionality as well as modified local structures alters properties such as magnetic moments, magnetic anisotropy, and more [5, 6]. While enormous progress has been made in magnetism, our understanding of magnetic anisotropy in thin film is far from completeness. In particular, the presence of substrate in practical fabrication, the role of magnetoelasticity as an interplay between magnetism and strain becomes important.

There have been numerous efforts to manipulate magnetic anisotropy. One way is the magnetoelastic coupling via substrate-induced lattice strain (ε) [7, 8], which is expected to have unprecedented impact. Changes in lattice constant via strain alters the interatomic distances between magnetic atoms, which subsequently modifies the interaction energy. The introduction of strain results in different magnetoelastic anisotropy (ME) [9-12]. As a result, spin reorientation transition (SRT) can emerge via strain, which is switching magnetization from in-plane to perpendicular direction or vice versa. Another factor is film thickness. Hence, SRT can be realized by choice of a substrate or by the variation of film thickness.

In this paper, theoretical investigation on strain driven SRT is presented. We provide a phenomenological model including magnetoelasticity and magnetic anisotropy in thin film limit. The influence of lattice strain on magnetic energy density is explicitly taken into account. Moreover, numerical calculations are performed for FePt and $Fe_{60}Co_{40}$ films in comparison with Fe film. These materials, candidates for magnetic storage devices, possess perpendicular magnetic anisotropy [13, 14]. We demonstrate that critical strain (ε_c) exists, where SRT emerges as a result of an interplay of magnetoelasticity and magnetic anisotropy. We show that $\varepsilon_c < 2$ % is required to achieve perpendicular magnetization in FePt and $Fe_{60}Co_{40}$ film with thickness less than 25 Å.

2. Results and Discussion

We consider a heterostructure as shown in Fig. 1, which consists of ultra-thin ferromagnetic (FM) film on top of thick nonmagnetic substrate. We further assume that the lateral strain of FM film is controllable by substrate and zero stress on the film surface [15]. Moreover, the stress and the strain fields inside the film are assumed homogeneous for single-domain FMs without misfit or dis-

*Co-corresponding author: Tel: +82-52-259-2331
Fax: +82-52-259-1693, e-mail: schong@mail.ulsan.ac.kr
Tel: +82-52-259-2325, Fax: +82-52-259-1693
e-mail: sonny@ulsan.ac.kr

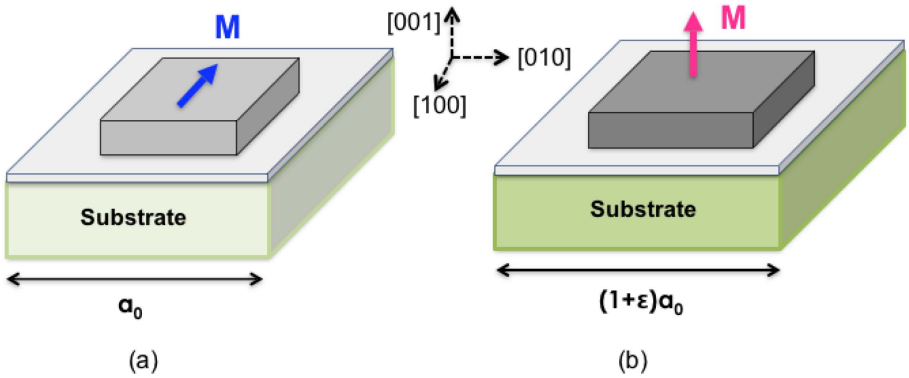

Fig. 1. (Color online) Schematic heterostructure of FM thin film on nonmagnetic substrate. (a) In-plane magnetization ($\vec{M}$) with lattice constant a_0 and (b) perpendicular $\vec{M}$ with strain (ε), lattice constant becomes $(1 + \varepsilon)\ a_0$.

location [15]. For simplicity, without loss of generality, FM film thickness (t_f) is regarded less than the material exchange length (l_{ex}), $t_f < l_{ex} = \sqrt{2A/\mu_o M_s^2}$, where A is the exchange coupling constant and M_s is the saturation magnetization [16]. Lateral dimension is assumed of nanoscale length to assure single-domain ground state. Strain (ε) is applied up to several percent on the magnetic layers through the substrate [17]. Temperature is taken well below the Curie temperature, whose effect is neglected.

Before we proceed theoretical approach, we remind that in real film with thickness larger than 100 Å or so, there is a delicate balance between shape and intrinsic MCA, which determines the preferred orientation of magnetization. The former prefers in-plane magnetization whereas the latter can be either in-plane or perpendicular one. As the film thickness reduces to a few Å, the interface contribution dominates over the bulk one [18]. This interface contribution is commonly attributed to the origin of SRT in thin film [19]. However, the presence of strain introduces another factor, magnetoelasticity. Non-negligible magnetoelasticity competes with aforementioned anisotropy [20, 21], where even subtle change in films may introduce SRT. In the following, we present our theoretical model.

We present total magnetic anisotropy energy (U) as sum of magnetoelastic (U_{MEL}), magnetocrystalline anisotropic (U_{MCA}), and demagnetization (U_{demag}) contributions,

$$U(\vec{m}) = U_{MEL}(\vec{m}) + U_{MCA}(\vec{m}) + U_{demag}(\vec{m}), \tag{1}$$

where each is expressed by polynomial expansion of $\vec{m}$, the unit vector or the directional cosines of magnetization. More specifically, the magnetoelastic energies (U_{MEL}) is expressed as

$$U_{MEL}(\vec{m}) = b_1\varepsilon_1\left[m_1^2 - \frac{c_{12}}{c_{11}}m_3^2\right] + b_1\varepsilon_2\left[m_2^2 - \frac{c_{12}}{c_{11}}m_3^2\right] + b_2\varepsilon_4 m_1 m_2 - \frac{b_1^2}{6c_{11}}m_3^2 + \left[\frac{b_1^2}{2c_{11}} - \frac{b_2^2}{2c_{44}}\right]m_3^2(m_1^2+m_2^2), \tag{2}$$

where ε_1, ε_2, ε_4 are lateral strains; b_1 and b_2 are the second order magnetoelastic coupling coefficients [22]; c_{11}, c_{22}, c_{44} are the elastic stiffness [11]. $U_{MEL}(\vec{m})$ is expanded up to the fourth order of m_i. The magnetocrystalline anisotropy energy, $U_{MCA}(\vec{m})$ is expressed as

$$U_{MCA}(\vec{m}) = K_1 m_1^2 m_2^2 + K_1 m_3^2(m_1^2+m_2^2) + K_2 m_1^2 m_2^2 m_3^2 + \frac{K_s}{t_f}m_3^2, \tag{3}$$

where K_1 is the fourth-order bulk magnetic anisotropy coefficient [23] mainly from the magnetoelastic and the elastic interactions under biaxial strain [20]; K_s is the second order of surface magnetic anisotropy and t_f is the thickness of FM film. K_2 is the sixth-order term of bulk magneto-anisotropy, which vanishes when $\vec{m}$ is either $m_1 = 1$ or $m_3 = 1$. Hence, K_2 and higher order terms are not included. The last term of Eq. (1) is the demagnetization energy, $U_{demag}(\vec{m})$, which reads

$$U_{demag}(\vec{m}) = \frac{1}{2}\mu_0 M_s^2(N_{11}m_1^2 + N_{22}m_2^2 + N_{33}m_3^2), \tag{4}$$

where N_{11}, N_{22}, N_{33} are the demagnetization factor [11].

We notice that U_{MEL} is linear in strains, ε_1 and ε_2, which can be either positive or negative depending on lattice mismatch by substrate. For biaxial lateral strain, $\varepsilon_1 = \varepsilon_2$, and by taking in-plane and perpendicular magnetization as $m_1 = 1$ and $m_3 = 1$, respectively, we find that $\varepsilon_c = \varepsilon_1 = \varepsilon_2$ exists, that is the critical strain when SRT emerges. Given $N_{11} \le N_{22}$ and $\varepsilon_4 = 0$, and using $K_1 = -b_1\,\varepsilon_1(1 + 2\frac{c_{12}}{c_{11}})$, the critical strain is obtained by minimizing U with respect to the magnetization,

$$\varepsilon_c = \frac{c_{11}}{b_1(c_{11}+2c_{12})}\left[\frac{1}{2}\mu_0 M_s^2(N_{33} - N_{11}) + \frac{K_s}{t_f} - \frac{b_1^2}{6c_{11}}\right]. \tag{5}$$

Table 1. Parameters used for numerical calculations for FePt, $Fe_{60}Co_{40}$, and Fe films. b_1 is the second order magnetoelastic coupling coefficients; M_s is the saturation magnetization; K_s is the second order of surface magnetic anisotropy; K_1 is the fourth order magnetic anisotropy coefficients; c_{11} and c_{22} are the elastic stiffness. All terms in Eqs. (2)-(5) describe energetics.

	b_1 (10^6 N/m^2)	M_s (10^6 A/m)	K_s (10^{-4} N/m^2)	K_1 (10^6 N/m^2)	c_{11} (10^{11} N/m^2)	c_{12} (10^{11} N/m^2)
FePt	-31.9[a]	0.7[b]	-10.0[c]	5.2[c]	3.0[c]	2.2[d]
$Fe_{60}Co_{40}$	-30.0[e]	1.3[f]	-13.0[g]	-0.01[h]	2.8[i]	1.4[i]
Fe	-3.3[j]	1.7[j]	-9.0[k]	0.05[j]	2.4[i]	2.4[i]

[a]Ref. **25**, [b]Ref. **26**, [c]Ref. **27**, [d]Ref. **28**, [e]Ref. **29**, [f]Ref. **30**, [g]Ref. **31**, [h]Ref. **32**, [i]Ref. **33**, [j]Ref. **24**, [k]Ref. **34**

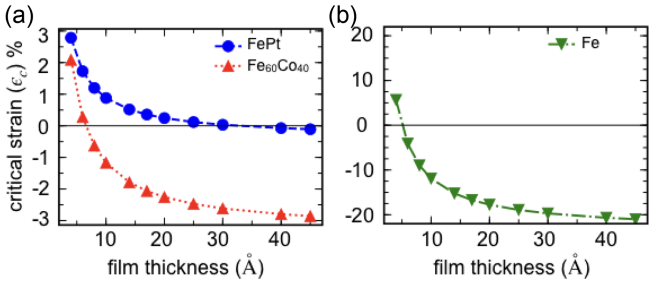

Fig. 2. (Color online) Calculated critical strain (ε_c) as a function of film thickness (t_f): (a) FePt (blue circle) and $Fe_{60}Co_{40}$ (red up-triangle), (b) Fe film (green down-triangle). Note the different vertical scales in (a) and (b).

The emergence of SRT is a result of interplay between anisotropy and magnetoelasticity. In thin film limit, as $N_{11} << N_{33}$, the first term of Eq. (5) is positive. The last term can be neglected compared to other terms. Indeed, ε_c can be either positive or negative depending on the relative signs of $\frac{1}{2}\mu_0 M_s^2(N_{33} - N_{11})$ and $\frac{K_s}{t_f}$. For $\varepsilon > \varepsilon_c$, magnetization becomes in-plane as $b_1 < 0$, whereas for $\varepsilon < \varepsilon_c$, magnetization becomes perpendicular. Moreover, ε_c is attributed solely to the interface anisotropy that shows large variation as film thickness changes [24].

For better quantitative understanding, numerical calculations are performed for FePt and $Fe_{60}Co_{40}$. Here, no particular substrate is considered. Instead, the role of substrate is parametrized by strain or lattice constant. Material parameters are listed in Table 1. The calculated critical strain (ε_c) as function of film thickness (t_f) for FePt, $Fe_{60}Co_{40}$, and Fe film is plotted in Fig. 2, where Fe film is shown for comparison purpose.

For FePt film, when $t_f < 25$ Å, perpendicular magnetization appears under 2% tensile strain. With increase in film thickness, the interface anisotropy decreases, and ε_c changes sign but remains small in magnitude. On the other hand, for $Fe_{60}Co_{40}$ film, similar to FePt, SRT emerges when $\varepsilon_c < 2$ % when $t_f < 15$ Å. As the film thickness increases, higher strain is required to switch magnetization from in-plane to perpendicular direction. Notably, ε_c changes sign at small thickness of a few Å, as both FePt and $Fe_{60}Co_{40}$ have huge first-order magnetoelastic and interface anisotropy coefficients. Furthermore, our results are compared with Fe film. Although, overall feature is similar to FePt and $Fe_{60}Co_{40}$ films, strain of $\varepsilon_c \sim 15$ % is necessary to realize SRT owing to small b_1 with $t_f \sim 15$ Å. As such, SRT in FePt and $Fe_{60}Co_{40}$ emerges around $\varepsilon_c \sim 2$ %, as a consequence of rather large b_1. More importantly, the value of 2 % is rather easily accessible in practical fabrications.

3. Conclusion

In conclusion, SRT is investigated using theoretical model, where the magnetoelasticity, the magnetocrystalline anisotropy, and the demagnetization are taken into account altogether. Our model accounts the heterostructure of thin FM film on nonmagnetic substrate. We have shown that SRT emerges at the critical strain (ε_c). For quantitative understanding, FePt and $Fe_{60}Co_{40}$ are numerically studied. Critical strain is 2 %, which is realistic in practical fabrication in contrast to Fe film. More specifically, the accessible critical strain of FePt and $Fe_{60}Co_{40}$ is consequence of large first-order magnetoelastic coefficient (b_1) and optimal saturation magnetization (M_s).

Acknowledgments

This work was supported by National Research Foundation of Korea (NRF) grant (NRF-2019R1I1A3A01059880).

References

[1] B. Heinrich and J. F. Cochran, Adv. Phys. **42**, 423 (1993).
[2] D. Weller, J. Stöhr, R. Nakajima, A. Carl, M. G. Samant, C. Chappert, R. Megy, P. Beauvillain, P. Veillet, and G. A. Held, Phys. Rev. Lett. **75**, 3752 (1995).
[3] U. Gradmann, J. Magn. Magn. Mater. **54**, 733 (1986).
[4] H. A. Dürr, G. Y. Guo, G. van der Laan, J. Lee, G. Lauhoff, and J. A. C. Bland, Science **277**, 213 (1997).
[5] G. Bochi, C. A. Ballentine, H. E. Inglefield, C. V. Thompson, and R. C. O'Handley, Phys. Rev. B 53, R1729(R) (1996).

[6] R. Thamankar, A. Ostroukhova, and F. O. Schumann, Phys. Rev. B 66, 134414 (2002).
[7] Y. Yahagi, B. Harteneck, S. Cabrini, and H. Schmidt, Phys. Rev. B **90**, 140405(R) (2014).
[8] Qurat-ul-ain, D. Odkhuu, S. H. Rhim, and S. C. Hong, Phys. Rev. B **101**, 214436 (2020).
[9] G. Binasch, P. Grünberg, F. Saurenbach, and W. Zinn, Phys Rev B **39**, 4828 (1989).
[10] S. A. Wolf, D. D. Awschalom, R. A. Buhrman, J. M. Daughton, S. von Molnár, M. L. Roukes, A. Y. Chtchelkanova, and D. M. Treger, Science **294**, 1488 (2001).
[11] L. D. Landau and E. M. Lifshitz, Electrodynamics of Continuous Media (Pergamon Press, Oxford, 1963).
[12] S. Ikeda, K. Miura, H. Yamamoto, K. Mizunuma, H. D. Gan, M. Endo, S. Kanai, J. Hayakawa, F. Matsukura, and H. Ohno, Nat. Mater. **9**, 721 (2010).
[13] S. Ikeda, J. Hayakawa, Y. M. Lee, F. Matsukura, Y. Ohno, T. Hanyu, and H. Ohno, IEEE Trans. Electron Devices. **54**, 991 (2007).
[14] J.-S. Noh, H. S. Kim, D. W. Chun, W. Y. Jeong, and W. Lee, Curr. Appl. Phys. **11**, S33 (2011).
[15] K. B. Vlasov, Zh. Eksp. Teor. Fiz. **38**, 889 (1960) [Sov. Phys.-JETP **11**, 642 (1960)].
[16] H. N. Bertram and C. Seberino, J. Magn. Magn. Mater. **193**, 388 (1999).
[17] A. Misra, M. Verdier, Y. C. Lu, H. Kung, T. E. Mitchell, M. Nastasi, and J. D. Embury, Scr. Mater. **39**, 555(1998).
[18] Y. Li, M. Farle, and K. Baberschke, J. Magn. Magn. Mater. **93**, 345 (1991).
[19] H. L. Meyerheim, D. Sander, R. Popescu, J. Kirschner, O. Robach, and S. Ferrer, Phys. Rev. Lett. **93**, 156105 (2004).
[20] K. Ha and R. C. O'Handley, J. Appl. Phys. **85**, 5282 (1999).
[21] J.-S. Lee, K.-B. Lee, Y. J. Park, T. G. Kim, J. H. Song, K. H. Chae, J. Lee, C. N. Whang, K. Jeong, D.-H. Kim, and S.-C. Shin, Phys. Rev. B **69**, 172405 (2004).
[22] C. Kittel, Rev. Mod. Phys. **21**, 541 (1949).
[23] N. A. Pertsev, Phys. Rev. B **78**, 212102 (2008).
[24] M. B. Stearns, in Magnetic Properties of Metals, edited by O. Madelung and Landolt-Börnstein, New Series, Group III, Vol. 19a (Springer-Verlag, Berlin, 1986).
[25] E. S. Leva, R. Valente, F. M. Tabares, M. V. Mansilla, S. Roshdestwensky, and A. Butera, Phys. Rev. B **82**, 144410 (2010).
[26] Y. Zhang, A. Kalitsov, J. Ciston, O. Mryasov, B. Ozdol, J. Zhu, S. Jain, B. Zhang, B. Livshitz, A. Chernyshov, A. Ajan, P. Dorsey, G. Bertero, R. Acharya, A. Greene, and S. Myers, AIP Adv. **8**, 125018 (2018).
[27] C. Feng, J. Zhao, F. Yang, K. Gong, S. Hao, Y. Cao, C. Hu, J. Zhang, Z. Wang, L. Chen, S. Li, L. Sun, L. Cui, and G. Yu, Sci. Rep. **6**, 20199 (2016).
[28] N. Nakamura, A. Uranishi, M. Wakita, H. Ogi, M. Hirao, and M. Nishiyama, Appl. Phys. Lett. **98**, 101911 (2011).
[29] R. Hall, J. Appl. Phys. **31**, S157 (1960).
[30] I. Jacobs, IEEE Trans. Magn. **21**, 1306 (1985).
[31] A. V. Azovtsev and N. A. Pertsev, Phys. Rev. Appl. **10**, 044041 (2018).
[32] G. Bayreuther, M. Dumm, B. Uhl, R. Meier, and W. Kipferl, J. Appl. Phys. **93**, 8230 (2003).
[33] J. P. Hirth, J. Lothe, and T. Mura, J. Appl. Mech. **50**, 476 (1983).
[34] A. Kozioł-Rachwał, W. Skowroński, T. Ślęzak, D. Wilgocka-Ślęzak, J. Przewoznik, T. Stobiecki, Q. H. Qin, S. van Dijken, and J. Korecki, J. Appl. Phys. **114**, 224307 (2013).